

Laser Direct Writing (LDW) of Graphene Patterns on Ceramic Utilizing a Flour Paste

Y-H. HUANG, S-J. NI AND L. LI*

Laser Processing Research Centre, School of Mechanical, Aerospace and Civil Engineering, The University of Manchester, Oxford Road, Manchester, M13 9PL, UK

Depositing patterned graphene on ceramic has been challenging due to multiple process steps required. In this paper a 355 nm wavelength ultraviolet (UV) picosecond laser was used to irradiate flour paste deposited on an Al_2O_3 ceramic substrate to form graphene without the need for a metallic precursor. The effect of process parameters including laser power, scanning speed, repetition rate and concentrations of the flour solution on graphene formation is investigated. The result shows that a concentration of 20% white wheat flour solution mixed with deionized water can ideally generate high quality graphene when processed with the picosecond laser at a 38 J/cm^2 laser fluence with 30 to 36 scan passes at a scanning speed of 100 mm/s. This low cost, one-step and versatile technique would have the potential for making high temperature electrical devices and sensors

Keywords: Picosecond laser, graphene, alumina, Al_2O_3 , plain white flour, ultraviolet (UV), laser direct writing (LDW), additive manufacturing (AM)

1 INTRODUCTION

Graphene is a two-dimensional (2-D) material that has an attractive mechanical property and superior thermal and electrical conductivities [1, 2]. Conventional methods of the graphene production include chemical vapor deposition (CVD) [3], mechanical exfoliation [4, 5] and graphene oxide reduction [5]. Around 1000°C temperature is typically required to synthesise large area, homogeneous crystalline graphene on copper or nickel foils

*Corresponding author: E-mail: lin.li@manchester.ac.uk

[6-11]. The high vacuum processing condition is typically required for the carbon precursor from high purity gases such as CH_4 , H_2 and Ar [12-14]. A suspended single layer graphene with zipper edge without any defect can be fabricated with a peeling process under a dust free condition. Microflakes of less than 200 μm limit wider industrial applications [15, 16]. Graphene oxide can be effectively produced through a hummer method with the evolution of $\text{NO}_2/\text{N}_2\text{O}_4$ toxic gasses and Mn_2+ waste water [17]. Graphene oxides have lower electrical conductivity than that of graphene due to the presence of defects from the reduction process [18]. A common challenge for CVD, mechanical exfoliation and graphene oxide reducing methods is that transfer of graphene to a substrate from Cu or Ni foils often result in relatively low adhesion [19].

Laser direct writing (LDW) is capable of locally treating materials at high temperatures over 1000°C and there is little thermal damage to the substrates with the precise control of laser energy and heat penetration depths [20, 21]. Previous graphene growth using a laser was mainly based on chemical vapour deposition (CVD). Carbon sources include carbon coating or hazardous gases, like CH_4 and H_2 at a 5:2 ratios. The selection of a metal precursor has a great impact on graphene growth, for instance, monolayer or bilayer graphene were achievable from Cu/Ni alloy as metal precursors [11, 22-26]; however, the use of a metal precursor requires a high temperature (over 1000°C) process and the issue about adhesion still exists on graphene transfer and metal removal processes.

Laser-induced graphene (LIG) could be generated with lignin or cellulose polymer directly without a metallic catalyst. A supercapacitor was directly written on a coconut shell by researchers at Rice University [27]. The aromatic group self-assembled under self-generation gas protection from amide or imide group of the lignin and cellulose by laser irradiation [28, 29]. The oven-dried wood includes about 18 to 30% lignin [29]. Other materials like coconut shells, cork as well as potato skins have approximately 25, 30 and 36% lignin, respectively, which have been used in previous research for graphene production [27]. LIG has been widely used for various applications, such as strain sensors, biosensors, supercapacitors and fuel cell. LIG grown on ceramic could be applied on high temperature electrical devices.

In this paper plain white flour from a supermarket was selected to be the carbon material. It is a powder that grounded from wheat. The main ingredient of flour is starch, which is a high polymer of glucose. It belongs to polysaccharides and consists of three different elements: C, H_2 and O_2 . The chemical form is $[(\text{C}_6\text{H}_{10}\text{O}_5)_n]$, which can be completely hydrolyzed to obtain glucose ($\text{C}_6\text{H}_{12}\text{O}_6$). It has a great potential to generate graphene with a high energy process with laser irradiation and it can be made into an ink mixed with deionized (DI) water or another liquid economically for depositing or printing on any substrates. A pulsed ultraviolet (UV)

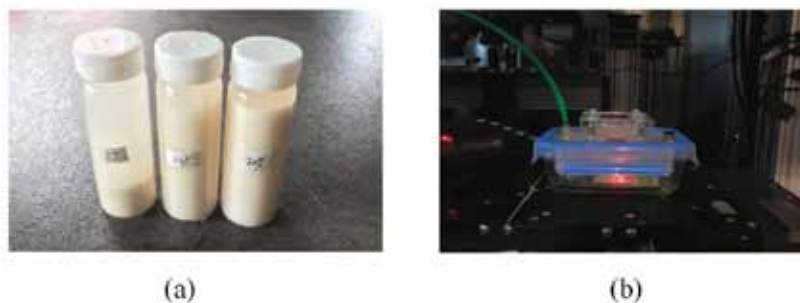


FIGURE 1
Photographs of (a) the 5%, 10% and 20% flour solutions and (b) the Ar gas protection system.

picosecond laser was used for the synthesis of N and S doped graphene on a polymer substrate with high photon energy and low thermal effect on the substrate [19].

2 MATERIALS AND EXPERIMENTAL PROCEDURES

As shown in Figure 1(a), the flour solution was prepared into 5, 10 and 20% concentration mixed with DI water. With increase of the flour concentration the solution gradually became sticky and it started to solidify when the concentration was over 20%. A flour coating of 100 to 150 μm in thickness on an Al_2O_3 ceramic substrate was prepared by drying the deposited solution under 100°C for 10 minutes.

LDW procedure was carried out under Ar gas protection in a gas shielding box, as shown in Figure 1(b), using a picosecond UV laser (GX-series Inno-Slab Laser; Edgewave, Inc.) with 355 nm wavelength, 10 ps pulse duration, 25 μm Gaussian beam and a 38 mJ/cm^2 laser fluence. The repetition number (or number of scanning passes) of processing was from 25 to 38 times.

The picosecond laser processed samples were analysed using Raman spectrometry with a single excitation wavelength of 514 nm. An optical microscope (VHX 5000: Keyence, Ltd.) and a field emission gun scanning electron microscope (FEG-SEM) (Sigma VP; Carl Zeiss AG). were used to understand the surface morphology changes.

3 RESULTS AND DISCUSSION

Initially, the picosecond laser processing was carried out in ambient conditions. There was no carbonization resulting from the picosecond laser processing, as is evident from Figure 2. The protective gas generated by the flour

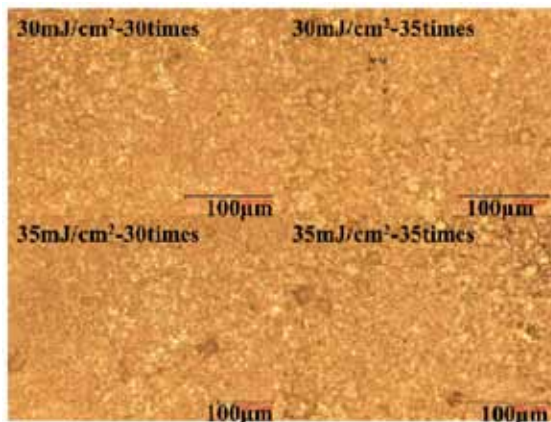


FIGURE 2

Optical micrographs of the picosecond laser irradiated 20% flour coating on the Al_2O_3 ceramic in open-air.

itself was not enough to prevent combustion of the flour. A high energy light input accelerated the oxidization reaction between the oxygen and carbonized glucose from decomposed flour irradiated by the picosecond laser beam; thus an Ar gas protection system was necessary for producing graphene from flour coating on the ceramic irradiated by the picosecond laser.

The carbonization showed black colour when the laser energy density was gradually increased to 30 mJ/cm^2 with 10 scanning passes and a 100 mm/s scanning speed. With a constant laser fluence of 30 mJ/cm^2 , more scanning passes from 10 to 35 times were applied in order to achieve graphitization of the flour [30]; however, the surface carbonized area became less. A porous structure and corresponding Raman spectroscopy result shown in Figure 3 demonstrate that laser fluence was below the graphitization threshold and so the laser fluence was raised to 38 mJ/cm^2 . With the increase of the laser fluence, the carbonization of the flour gradually enhanced with the rise of the G peak, as displayed in Figure 3 and Figure 4.

Graphitization occurred with the growth of 2D peak (see Figure 5), which demonstrated the nano-crystallization growth with more repetition time [31]. Then, the ratio of 2D peak and G peak grew to $\frac{3}{4}$; that is, 3 to 4 layers of graphene [19] when the number of passes was 30, as shown in Figure 5. The decrease of electrical resistance measured from more than $200 \text{ }\Omega/\text{square}$ to around $50 \text{ }\Omega/\text{square}$ by a multimeter also demonstrated the increase of the degree of graphitization. The graphene growth induced higher momentum of charge carrier through 2π orbitals, which was able to suppress electron back scattering [32]. The effect of graphitization from the laser irradiation was saturated when the number of passes was more than 30

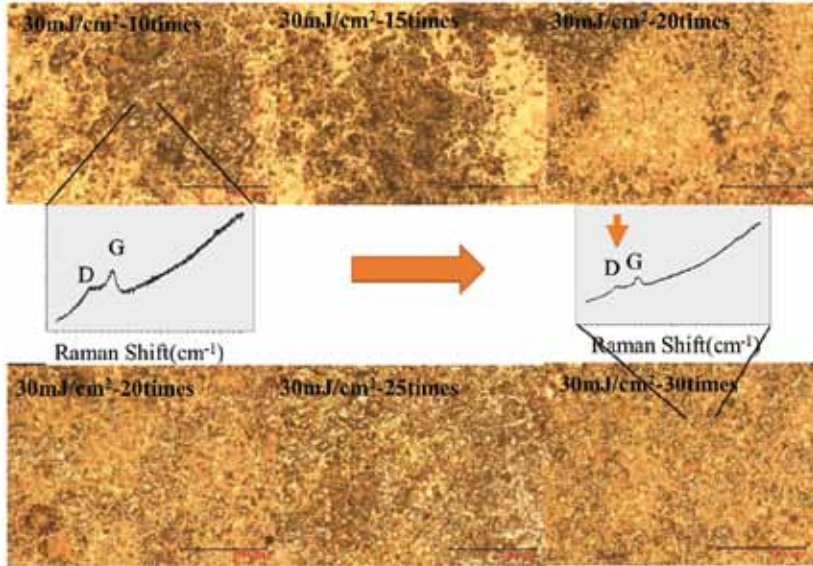


FIGURE 3

The Raman spectroscopy results and optical micrographs of the surface morphology changes from 20% flour coating on the Al_2O_3 ceramic under Ar gas protection irradiated with the picosecond laser at 30 mJ/cm^2 for 10 to 35 times.

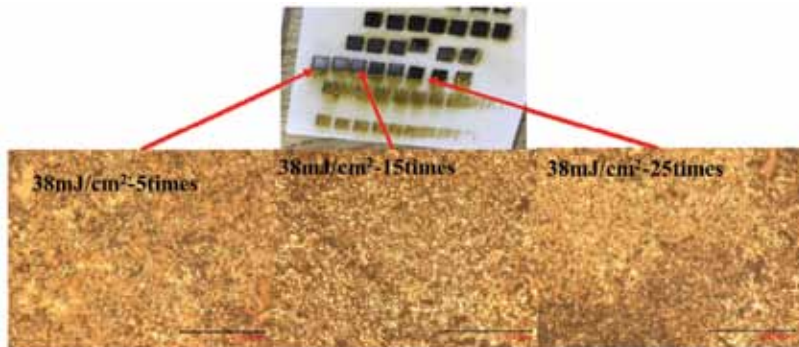


FIGURE 4

Photograph (upper) and optical micrographs (lower) showing visible and morphology changes of the 20% flour coating on the Al_2O_3 ceramic processed with the picosecond laser at 38 mJ/cm^2 laser fluence for 5 to 25 times under Ar gas protection.

to 32. As is evident in Figure 5, the increase of ratio between D and G peak from 30 to 34 repetition times demonstrated damages from the over irradiated process, which resulted in more porous surface structures. The 2D peak was impacted and dropped with the over irradiation. The over irradi-

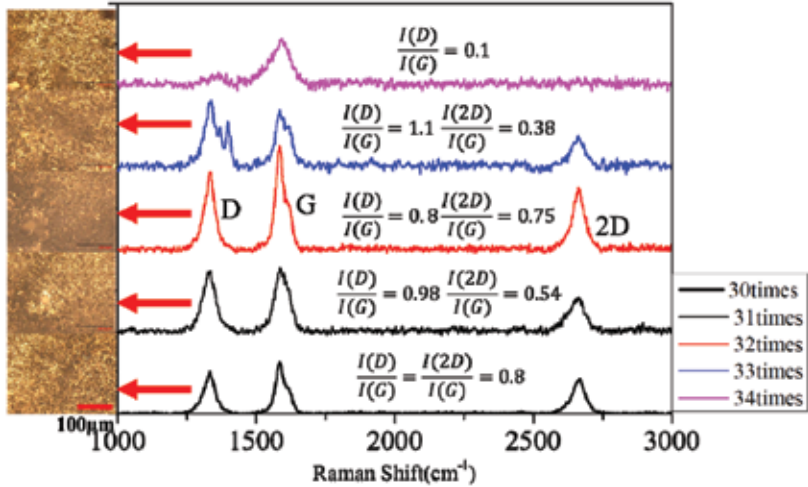


FIGURE 5

Raman spectroscopy result of 20% flour coating on the Al_2O_3 ceramic processed with the pico-second laser at 38 mJ/cm^2 laser fluence under Ar gas protection for 30 to 35 times (right-hand side) and corresponding optical micrographs showing the surface morphology change (left-hand side).

ated process occurred when the laser fluence was over 38 mJ/cm^2 . The high ratio of ablation and graphitization structure breaking became the primary result from excessive energy deposited; therefore, the graphene was eventually transferred to amorphous carbon when the number of passes increased to 35. There were no 2D peak or short D peak presented from the Raman spectroscopy result shown in Figure 5.

Graphene direct laser writing was achieved at 38 mJ/cm^2 laser processing for 30 times under Ar gas protection, as shown in Figure 6. It would have great potential to pattern electrical circuits on ceramic substrates for fabricating high thermal resistance electrical devices and temperature sensors [33].



FIGURE 6

Photograph showing actual graphene LDW on an Al_2O_3 ceramic substrate.

4 CONCLUSIONS

We have demonstrated a low cost, flexible and highly efficient method to produce graphene patterns on an Al_2O_3 ceramic substrate without metallic coatings using laser direct writing (LDW). At 38 mJ/cm^2 fluence pulsed ultraviolet (UV) picosecond laser irradiation of 30 passes, one can transfer flour/water solution into conductive graphene of 2 to 3 layers, processed in an Ar gas environment. This presents a potential for the manufacture of high thermal resistance electrical devices or temperature sensors.

REFERENCES

- [1] Zhen Z. and Zhu H.W. Structure and properties of graphene. in Zhu H-W., Xu Z-P., Xie D. and Fang Y. (Eds.) *Graphene: Fabrication, Characterizations, Properties and Applications*. New York: Elsevier. 2018:
- [2] Ferrari A.C. and Basko D.M. Raman spectroscopy as a versatile tool for studying the properties of graphene. *Nature Nanotechnology* **8**(4) (2013), 235-246.
- [3] Reina A., Jia X., Ho J., Nezich D., Son H., Bulovic V., Dresselhaus M.S. and Kong J. Large area, few-layer graphene films on arbitrary substrates by chemical vapor deposition. *Nano Letters* **9**(1) (2009), 30-35.
- [4] Kim K.S., Zhao Y., Jang H., Lee S.Y., Kim J.M., Kim K.S., Ahn J-H., Kim P., Choi J-Y., and Hong B.H. Large-scale pattern growth of graphene films for stretchable transparent electrodes. *Nature* **457** (2009), 706.
- [5] Ong W-J., Tan L-L., Chai S-P., Yong S-T. and Mohamed A.R. Surface charge modification via protonation of graphitic carbon nitride (g- C_3N_4) for electrostatic self-assembly construction of 2D/2D reduced graphene oxide (rGO)/g- C_3N_4 nanostructures toward enhanced photocatalytic reduction of carbon dioxide to methane. *Nano Energy* **13** (2015), 757-770.
- [6] Cho J.H., Gorman J.J., Na S.R. and Cullinan M. Growth of monolayer graphene on nanoscale copper-nickel alloy thin films. *Carbon* **115** (2017), 441-448.
- [7] Chae S.J., Gunes F., Kim K.K., Kim E.S., Han G.H., Kim S.M., Shin H.J., Yoon S.M., Choi J.Y., Park M.H., Yang C.W., Pribat D. and Lee Y.H. Synthesis of large-area graphene layers on poly-nickel substrate by chemical vapor deposition: wrinkle formation. *Advanced Materials* **21**(22) (2009), 828039
- [8] Chen S.S., Cai W.W., Piner R.D., Suk J.W., Wu Y.P., Ren Y.J., Kang J.Y. and Ruoff R.S. Synthesis and characterization of large-area graphene and graphite films on commercial Cu-Ni alloy foils. *Nano Letters* **11**(9) (2011), 3519-3525.
- [9] Li X.S., Cai W.W., An J.H., Kim S., Nah J., Yang D.X., Piner R., Velamakanni A., Jung I., Tutuc E., Banerjee S.K., Colombo L. and Ruoff R.S. Large-area synthesis of high-quality and uniform graphene films on copper foils. *Science* **324**(5932) (2009), 1312-1314.
- [10] Reina A., Jia X.T., Ho J., Nezich D., Son H.B., Bulovic V., Dresselhaus M.S. and Kong J. Large area, few-layer graphene films on arbitrary substrates by chemical vapor deposition. *Nano Letters* **9**(1) (2009), 30-35.
- [11] Ye X., Lin Z., Zhang H., Zhu H. and Zhong M. Laser controllable growth of graphene via Ni-Cu alloy composition modulation. *Lasers in Manufacturing and Materials Processing* **2**(4) (2015), 219-230.
- [12] Ismac, A., Druzgalski C., Penwell S., Schwartzberg A., Zheng M., Javey A., Bokor J. and Zhang Y.G. Direct chemical vapor deposition of graphene on dielectric surfaces. *Nano Letters* **10**(5) (2010), 1542-1548.
- [13] Kumar A., Khan S., Zulfeqar M., Harsh and Husain M. Low temperature synthesis and field emission characteristics of single to few layered graphene grown using PECVD. *Applied Surface Science* **402** (2017), 161-167.

- [14] Fan L.S., Xiong W., Gao Y., Park J., Zhou Y.S., Jiang L. and Lu Y.F. Laser direct writing graphene patterns on SiO₂/Si substrates. *Proceedings of the SPIE: Laser-Based Micro- and Nanopackaging and Assembly VII* **8608** (2013), 806080J.
- [15] Bunch J.S., van der Zande A.M., Verbridge S.S., Frank I.W., Tanenbaum D.M., Parpia J.M., Craighead H.G. and McEuen P.L. Electromechanical resonators from graphene sheets. *Science* **315**(5811) (2007), 490-493.
- [16] Hyun C., Yun J., Cho W.J., Myung C.W., Park J., Lee G., Lee Z., Kim K. and Kim K.S. Graphene Edges and beyond: temperature-driven structures and electromagnetic properties. *ACS Nano* **9**(5) (2015), 4669-4674.
- [17] Chen J., Yao B., Li C. and Shi G. An improved Hummers method for eco-friendly synthesis of graphene oxide. *Carbon* **64** (2013), 225-229.
- [18] Eda G., Fanchini G. and Chhowalla M. Large-area ultrathin films of reduced graphene oxide as a transparent and flexible electronic material. *Nature Nanotechnology* **3** (2008), 270.
- [19] Huang Y., Zeng L., Liu C., Zeng D., Liu Z., Liu X., Zhong X., Guo W. and Li L. Laser direct writing of heteroatom (N and S)-doped graphene from a polybenzimidazole ink donor on polyethylene terephthalate polymer and glass substrates. *Small* **14**(44) (2018), 1803143.
- [20] Gautam G.D. and Pandey A.K. Pulsed Nd:YAG laser beam drilling: A review. *Optics & Laser Technology* **100** (2018), 183-215.
- [21] Lin J., Peng Z.W., Liu Y.Y., Ruiz-Zepeda F., Ye R.Q., Samuel E.L.G., Yacaman M.J., Yakobson B.I. and Tour J.M. Laser-induced porous graphene films from commercial polymers. *Nature Communications* **5** (2014), 8.
- [22] Park J.B., Xiong W., Xie Z.Q., Gao Y., Qian M., Mitchell M., Mahjouri-Samani M., Zhou Y.S., Jiang L. and Lu Y.F. Transparent interconnections formed by rapid single-step fabrication of graphene patterns. *Applied Physics Letters* **99**(5) (2011), 053103.
- [23] Park J.B., Xiong W., Gao Y., Qian M., Xie Z.Q., Mitchell M., Zhou Y.S., Han G.H., Jiang L. and Lu Y.F. Fast growth of graphene patterns by laser direct writing. *Applied Physics Letters* **98**(12) (2011), 123109.
- [24] Jiang J., Lin Z., Ye X.H., Zhong M.L., Huang T. and Zhu H.W. Graphene synthesis by laser-assisted chemical vapor deposition on Ni plate and the effect of process parameters on uniform graphene growth. *Thin Solid Films* **556** (2014), 206-210.
- [25] Xiong W., Zhou Y.S., Jiang L.J., Sarkar A., Mahjouri-Samani M., Xie Z.Q., Gao Y., Ianno N.J., Jiang L. and Lu Y.F. Single-step formation of graphene on dielectric surfaces. *Advanced Materials* **25**(4) (2013), 630-634.
- [26] Xiong W., Zhou Y.S., Hou W.J., Jiang L.J., Gao Y., Fan L.S., Jiang L., Silvain J.F. and Lu Y.F. Direct writing of graphene patterns on insulating substrates under ambient conditions. *Scientific Reports* **4829** (2014), 04892.
- [27] Daud W.M.A.W. and Ali W.S.W. Comparison on pore development of activated carbon produced from palm shell and coconut shell. *Bioresource Technology* **93**(1) (2004), 63-69.
- [28] Lin J., Peng Z., Liu Y., Ruiz-Zepeda F., Ye R., Samuel E.L.G., Yacaman M.J., Yakobson B.I. and Tour J.M. Laser-induced porous graphene films from commercial polymers. *Nature Communications* **5** (2014), 5714.
- [29] Ye R., Chyan Y., Zhang J., Li Y., Han X., Kittrell C. and Tour J.M. Laser-induced graphene formation on wood. *Advanced Materials* **29**(37) (2017), 1702211.
- [30] Budde H., Coca-López N., Shi X., Ciesielski R., Lombardo A., Yoon D., Ferrari A.C., and Hartschuh A. Raman radiation patterns of graphene. *ACS Nano* **10**(2) (2016), 1756-1763.
- [31]
- [32] Tuinstra F. and Koenig J.L. Raman spectrum of graphite. *The Journal of Chemical Physics* **53**(3) (1970), 1126-1130.
- [33] Fuhrer M.S., Lau C.N. and MacDonald A.H. Graphene: Materially better carbon. *MRS Bulletin* **35**(4) (2011), 289-295.
- [34] Davaji B., Cho H.B., Malakoutian M., Lee J-K., Panin G., Kang T.W. and Lee C.H. A patterned single layer graphene resistance temperature sensor. *Scientific Reports* **7**(1) (2017), 8811.